LUNAR H_2O/OH^- DISTRIBUTIONS: REVISED INFRARED SPECTRA FROM IMPROVED THERMAL CORRECTIONS. J. L. Bandfield[1], C. S. Edwards[2], M. J. Poston[3], and R. L. Klima[4], [1]Space Science Institute (jbandfield@spacescience.org), [2]U.S. Geological Survey Flagstaff Field Center, [3]California Institute of Technology, [4]Applied Physics Laboratory, Johns Hopkins University.

Introduction: There has been considerable interest in the spectral response of the lunar surface near 2.8 and 2.95 μm, where OH^- and H_2O have strong absorptions. Previous studies have identified these absorptions with variable strengths across the lunar surface [*1–7*]. In particular, the absorptions have been found to be most prominent at higher latitudes and at early and late local times (e.g., [*1–2*]), leading investigators to consider a dynamic environment where much of the OH^-/H_2O migrates around the Moon on diurnal timescales (e.g., [*1,4,8–10*]).

The accuracy of these results are highly dependent on the accounting and removal of emitted radiance from the measured spectra beyond ~2 μm. Current emitted radiance corrections for lunar spectral data assume an isothermal surface and/or a predictive spectral continuum (e.g., [*11–12*]). These corrections have an advantage of being relatively simple to implement, without additional models or datasets. However, the assumptions inherent in these corrections can lead to a significant mis-estimation of the emitted radiance. For example, surface temperatures and emitted radiance are systematically underestimated in the thermally corrected Chandrayaan-1 Moon Mineralogy Mapper (M^3) Level 2 radiance data.

To understand and accurately model thermal emission from the lunar surface, we must understand the thermophysical properties of the surface. The spatial, angular, and temporal variations of temperature reflect regolith properties, such as particle size distribution and density. These properties represent a delicate balance of lunar surface processes that produce a highly structured regolith over time (e.g., [*13–16*]).

In particular, the effects of surface roughness on thermal emission have been recognized as a dominant factor in the thermal emission of airless bodies, including the Moon [*17–18*]. This understanding has come with the collection of more precise and systematic datasets, and the development of increasingly sophisticated models. The current thermal corrections applied to these data are insufficient in part because they do not account for these effects.

As a result of surface roughness, lunar surface temperatures derived from NIR measurements will commonly show brightness temperatures that are much higher than the average surface temperature in the measurement field of view (Fig. 1). In addition, the brightness temperature will not be constant with respect to wavelength, even within limited spectral ranges. Properly accounting for anisothermality and correcting for this emitted radiance is crucial for the characterization of the 3 μm OH^- and H_2O absorptions.

Methods and Data: For this work, we use a simple radiative equilibrium model to predict the temperature of each surface facet [*19*]. To model roughness, we use a Gaussian distribution of slopes similar to that of [*20*]. This reduces the surface slopes/roughness to a single parameter (RMS slope distribution), while maintaining reasonable fidelity to natural surfaces. Using the modeled temperatures for each slope/azimuth combination and slope distribution, the mixture of Planck radiances are calculated in proportion to their contribution to the measurement field of view. The resulting modeled spectral radiance has been compared with Lunar Reconnaissance Orbiter (LRO) Diviner Radiometer measurements. These results indicate that typical lunar regolith surfaces are consistent with a mm to cm-scale RMS slope distribution of 20–25° [*19*].

The correction of M^3 data using the output of the roughness thermophysical model (radiance as a function of wavelength) is relatively straightforward. We assume a Lambertian surface and that Kirchoff's Law applies ($\varepsilon = 1 - R$). The examples shown here assume a surface slope distribution of 20° RMS, similar to typical lunar regolith [*19*].

Results: The initial application of the roughness model for the removal of thermal contributions from M^3 data has a dramatic effect on the resulting spectra (Fig. 2). At wavelengths greater than ~2.5 μm, the

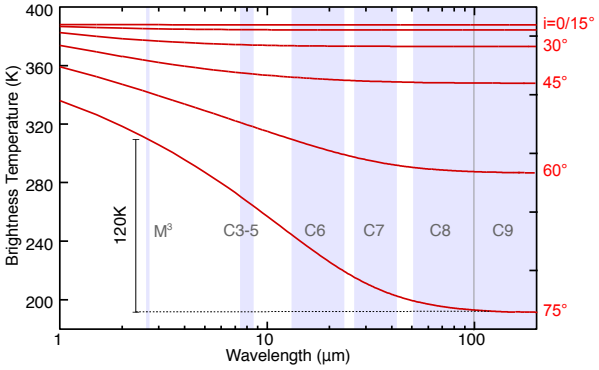

Fig. 1. Lunar brightness temperatures as a function of wavelength for a typical regolith surface (Albedo = 0.10, RMS slopes = 20°). Anisothermality increases with increasing angles of solar incidence (i). C3–9 indicate wavelength coverage of LRO Diviner spectral channels and M^3 indicates the wavelength used for the thermal emission correction of M^3 Level 2 data.

corrected I/F spectra show a prominent negative slope with increasing wavelength. Even assuming an isothermal surface at typical lunar surface temperatures, the strong downturn is present. By comparison, the M^3 Level 2 thermally corrected data appear to be severely under-corrected. The modeled brightness temperatures are significantly higher than the M^3 Level 2 derived surface temperature (Fig. 2), resulting in a much higher estimated thermal emission contribution and, consequently, lower I/F values in the isothermal and rough surface corrected data.

Diviner measurements collected over the same surface at similar solar incidence and emission angles are in good agreement with the brightness temperatures predicted by the roughness model at 3 μm, with a trend of increasing brightness temperatures towards shorter wavelengths. The newly corrected data have a prominent downturn in the spectral data at wavelengths greater than ~2.7–2.8 μm that is not apparent in the M^3 Level 2 thermally corrected data.

A similar pattern is present at a variety of latitudes and solar incidence angles (Fig. 3). The M^3 Level 2 thermally corrected data show increasingly prominent 2.8–3.0 μm absorptions at high angles of solar incidence. By contrast, the rough surface thermal correction predicts much higher brightness temperatures and the corrected spectra show a prominent downturn in reflectance beyond 2.7 μm at all angles of solar incidence. This downturn appears at all latitudes, including near midday at the equator.

Conclusions: The initial results described here show that the incorporation of thermal roughness modeling can cause a dramatic change in both the shape and distribution of the ~3 μm absorption across the lunar surface. This is likely to result in a significantly revised interpretation of its source and the processes that lead to its occurrence. For instance, *6, 21–22* have identified OH^-, with evidence supporting a magmatic source. Concentrations of OH^- and H_2O in minerals and fluid inclusions can be high enough to be detectable via spectroscopic measurements (e.g., [*8*]). Some of these forms of bound H_2O may not be nearly as temperature dependent as adsorbed H_2O. The lack of variation in the newly corrected spectral data may negate the need to identify a temperature dependent formation mechanism for lunar H_2O.

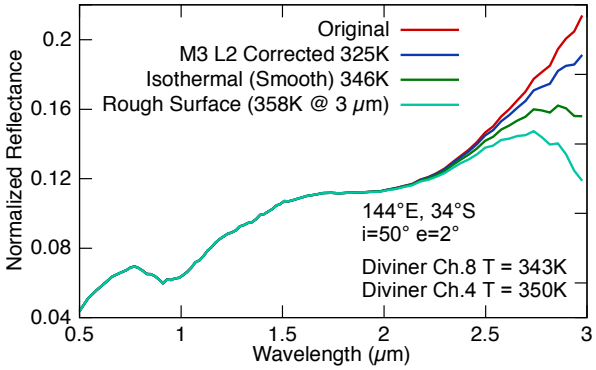

Fig 2. The effect of surface roughness on the thermal correction of M^3 data. The apparent depression in reflectance beyond 2.5 μm becomes more prominent with increasing roughness.

References: [1] Pieters C.M. et al. (2009) *Science*, 56810.1126/science.1178658. [2] Sunshine J.M. et al. (2009) *Science*, 56510.1126/science.1179788. [3] Clark R.N. (2009) *Science*, 56210.1126/science.-1178105. [4] McCord T.B. et al. (2011) *JGR*, 10.1029 / 2010JE003711. [5] Kramer G.Y. et al. (2011) *JGR*, 10.1029/2010JE003729. [6] Klima R.L. et al. (2013) *Nat. Geo.*, 10.1038/ngeo1909. [7] Li S. and Milliken R.E. (2013) *LPSC*, 44, 1337. [8] Dyar M.D. et al. (2010) *Icarus*, 10.1016/j.icarus.2010.02.014. [9] Hibbits, C.A. et al. (2011) *Icarus*, 10.1016/j.icarus.-2011.02.015. [10] Poston M.J. (2013) *JGR*, 10.1029/-2012JE004283. [11] Clark R.N. (2011) *JGR*, 10.-1029/2010JE003751. [12] Groussin O. (2007) *Icarus*, 10.1016/j.icarus.2012.10.003. [13] Keihm S.J. (1973) *EPSL*, 10.1016/0012-821X(73)90084-8. [14] Vasavada A.R. et al. (2012) *JGR*, 010.1029/2011JE003987. [15] Hayne P.O. et al. (2013) *LPSC*, 44, 3003. [16] Ghent, R.R. et al. (2014) *Geology*, 10.1130/G35926.1. [17] Lagerros J.S.V. (1998) *Astron. & Astrophys.*, *332*, 1123 -1132. [18] Davidsson B.J. et al. (2015) *Icarus*, 10.1016/j.icarus.2014.12.029. [19] Bandfield J.L. et al. (2015) *Icarus*, 10.1016/j.icarus.2014.11.009. [20] Helfenstein P. and Shepard M.K. (1999) *Icarus*, 10.-1006/icar.1999.6160. [21] Saal A.E. et al. (2008) *Nature*, 10.1038/nature07047, 192-U138. [22] McCubbin F.M. et al. (2010) *PNAS*, 10.1073/pnas.-1006677107.

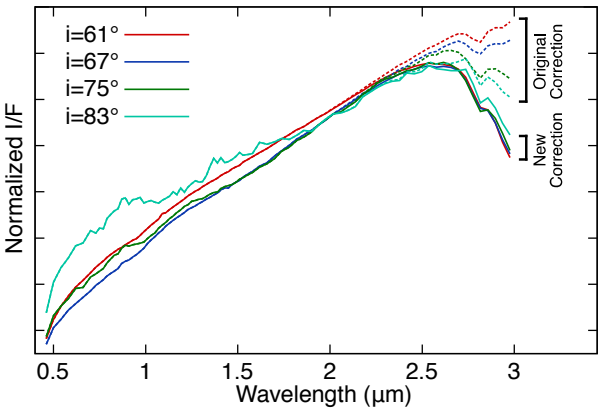

Fig. 3. Original (dashed) and roughness model (solid) thermally corrected M^3 data for a range of solar incidence angles (i). The roughness model correction shows a much more prominent downturn in reflectance beyond ~2.7 μm and the systematic variation with solar incidence is no longer present.